

## TDR permittivity measurements of dielectric films

J. Obrzut<sup>1</sup> and R. Nozaki<sup>2</sup>

<sup>1</sup> Polymers Division, National Institute of Standards and Technology, Gaithersburg, MD 20899

<sup>2</sup> Division of Physics, Graduate School of Science, Hokkaido University, Sapporo 060-0810, Japan.

**Abstract** – We describe a time-domain reflectometry (TDR) technique to measure the dielectric permittivity of film materials with enhanced dielectric constant. The test specimen consists of a planar capacitor terminating coaxial waveguide. The complex permittivity is obtained from analysis of the incident and the reflected voltage waves. In order to improve accuracy at higher frequencies, we introduced a propagation term correcting the lumped element model. The applicability of the method has been verified at frequencies from 100 MHz to 10 GHz on several polymer composite films, 8  $\mu\text{m}$  to 100  $\mu\text{m}$  thick, having a dielectric constant ranging from 3.5 to 40. When compared to other techniques, TDR provides a more intuitive and direct insight into capacitance density and impedance characteristics, which is useful in high-frequency characterization of materials for embedded capacitance applications.

**Keywords** – TDR, high frequency measurements, dielectric materials

### I. INTRODUCTION

Most of the existing microwave methods of permittivity measurement are not feasible for thin films and small dimensions. For example, test procedures utilizing a lumped element are limited to the frequency range below 1 GHz [1] while those based on microwave cavities, or microstrip resonators require rather large samples [2-4]. In the resonant techniques, the radiation losses and non-optimized coupling conditions are common sources of errors in the measured permittivity. Additional difficulties arise from electrical requirements, which for high dielectric constant films can be realized only with tiny patterns and highly conducting metal traces that are hard to fabricate and evaluate. Thus the resonant techniques usually utilize a unique sample configuration useful for certain type of materials at specific frequencies [5-6]. In contrast, time-domain reflectometry (TDR) offers broadband measurements. When compared to frequency domain techniques, TDR provides a more intuitive and direct insight into specimen characteristics, which is very convenient in materials characterization and development of new testing procedures. The TDR method has been used to determine an effective dielectric constant of printed circuit board materials by means of a time delay of a co-planar transmission line [7]. In difference, our TDR measurement of complex permittivity is based on analysis of the total reflection pattern produced by the dielectric specimen terminating a coaxial line. This approach has been widely used to characterize the dielectric properties of liquids in

variety of configurations. Among them, a lumped capacitance termination corresponds to the smallest cross-section of the specimen, for which approximate expression for the input admittance has been established assuming quasi-static conditions [8]. At higher frequencies thin film specimens require, however, a more accurate solution to account for non-stationary electric fields and wave propagation in the sample section [9, 10].

We examined the applicability of the TDR technique to permittivity measurements of dielectric materials with enhanced dielectric constant for embedded passive device and embedded capacitance applications.

### II. PROBLEM DEFINITION

The experimental arrangement under consideration is shown in Figure 1. A dielectric film of thickness  $t$  is placed at the end of the APC-7 coaxial line of impedance  $Z_0 = 50 \Omega$  and length  $l$ , and terminated by a short. When a voltage step of amplitude  $V_i$  is launched into the line, the wave is partially reflected back at the reference plane, and then is added to the

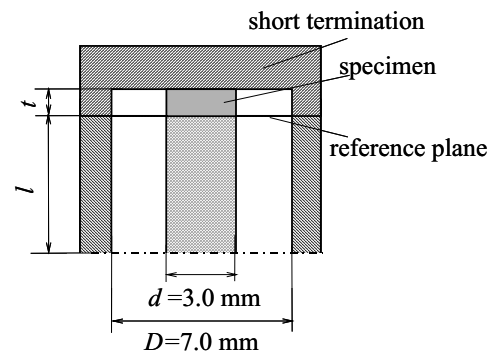


Fig. 1. Sample configuration

original incident wave after a delay  $\tau_0 = 2l/v_p$ , where  $v_p$  denotes the velocity of propagation in the coaxial line.

The shape of the reflected wave  $V_r$  depends on the nature and magnitude of mismatch between the line impedance  $Z_0$  and impedance of the termination. Examples of the load effect on the shape of TDR responses are illustrated in Figure 2. In Figure 2a the incident wave is reflected at an open circuit. Since both the incident wave and the reflected wave are in phase,  $V_r = V_i$ , they combine after the time  $\tau_0$ , resulting in the reflected amplitude of  $2V_i$ . In comparison, the reflected wave at a short circuit is out of phase by  $180^\circ$  in respect to the incident wave,  $V_r = -V_i$ , and thus the initial

voltage step returns to zero after the time  $\tau_0$ , as it is illustrated in Figure 2b. The TDR response produced by a 250 mV step reflected at air-filled capacitance having gap of 10  $\mu\text{m}$  and 2  $\mu\text{m}$ , is shown in plots c and d of Figure 2 respectively. Example response from a 100  $\mu\text{m}$  thick specimen, having at 5 GHz a dielectric constant of about 36 is shown in Figure 2e. In all three illustrations the line is terminated with a lumped capacitance, the resulting reflection has a rising in time exponential shape. The electrical circuit corresponds to a complex shunt resistance – capacitance ( $R$ - $C$ ) termination for which the transient voltage can be described by equation (1).

$$V_r(\tau) = V_i \left[ \left(1 + \frac{R - Z_0}{R + Z_0}\right) \left(1 - \exp\left(-\frac{\tau}{T}\right)\right) \right] \quad (1)$$

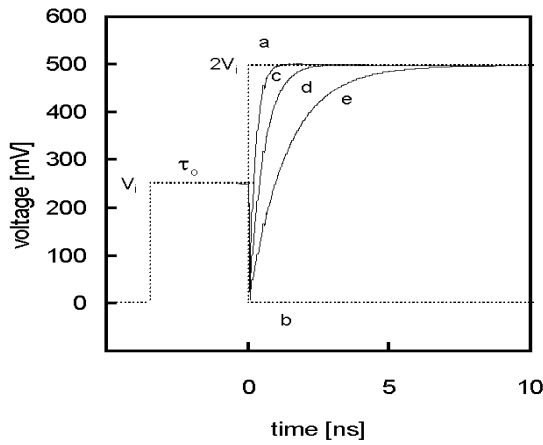


Fig. 2. – Dependence of the TDR response on the termination. (a) open; (b) short; (c) 10  $\mu\text{m}$  air-gap; (d) 2  $\mu\text{m}$  air-gap; (e) 100  $\mu\text{m}$  thick film having dielectric constant of 36.

where:  $T = \frac{Z_0 R}{Z_0 + R} C$  is the relaxation charging time,  $R$  is

the resistance and  $C$  is the capacitance of the specimen. For simplicity, the time parameter in equation (1) is chosen to be zero when the reflected wave arrives back to the detector,  $\tau$  at  $\tau_0 = 0$ . It is seen that at time zero the  $R$ - $C$  load appears as a short circuit. Then the voltage builds up across the capacitance increasing its impedance until it effectively becomes an open circuit. From equation (1) the total voltage at  $\tau = \infty$  is  $(1 + (R - Z_0)/(R + Z_0)) V_i$ , which approaches  $2V_i$  when  $R$  becomes infinitely large. This corresponds to a dielectric with negligible loss, such as an air-gap terminating the transmission line as shown in Figure 2, plots c and d.

The circuit expression (1) is better suited for calculation of the expected electrical behavior for a given dielectric rather than for evaluation of permittivity from the experimental voltage waves. In fact, an explicit solution for permittivity cannot be obtained even for the simplest dielectric relaxation mechanism since it is simultaneously entangled with

reflection coefficient and propagation functions. Thus only approximate solutions are possible.

A time dependent voltage across the sample,  $V(\tau)$ , can be related to a time dependent charge and the geometric capacitance through an appropriate response function which links the reflected wave with the dielectric permittivity,  $\epsilon^*$ , of the specimen. Evaluation of  $\epsilon^*$  from the observed reflected voltage wave,  $V_r$ , involves Laplace transformation of the response function obtained in the time domain and the propagation equation for the coaxial line, with appropriate boundary conditions. Usually, a thin film capacitance at the end of the coaxial line has been treated as a primary capacitance with a fringing field capacitance without electrical length [8]. Such treatment becomes inaccurate at short times (high frequencies) for a finite film, which represents a radial waveguide of cylindrical cross-section. The incoming wave through the coaxial line is partially reflected at the impedance discontinuity while some portion of it propagates inside the specimen section. If  $d \ll t$ , then the primary propagation mode satisfying the boundary conditions in the specimen section is associated with the diameter rather than the thickness of the specimen.

Neglecting the residual inductance, the input admittance of the specimen section can be described as follows [7]:

$$Y_{in} = j\omega C_p \epsilon_r^* [x \cot(x)]^{-1} \quad (2)$$

where:  $x = \frac{\omega a}{c} \sqrt{\epsilon_r^*}$  accounts for the wave propagation,

$a$  is the propagation length,  $\epsilon_r^*$  is the relative complex permittivity of the specimen,  $\omega$  is an angular frequency,  $c$  is the velocity of propagation in vacuum, and  $C_p$  represents a geometric capacitance of the specimen filled with air.

On the other hand, the input admittance can be expressed by measurable TDR waves:

$$Y_{in} = G_0 \frac{V_i(j\omega) - V_r(j\omega)}{V_i(j\omega) + V_r(j\omega)} \quad (3)$$

where:  $V_i(j\omega)$  and  $V_r(j\omega)$  are the Laplace transforms of the incident and the reflected waves, and  $G_0 = 1/50$  [ $1/\Omega$ ] is the characteristic conductance of the coaxial line.

By combining equations (2) and (3) we obtain expression (4) for complex permittivity  $\epsilon^*$  as a function of measurable incident and reflected waves,  $V_i$  and  $V_r$ , which are referenced at the time  $\tau_0$  as it is shown in Figure 2:

$$\epsilon^* = \frac{c}{j\omega(gd)} \frac{V_i(j\omega) - V_r(j\omega)}{V_i(j\omega) + V_r(j\omega)} f \quad (4)$$

In (4)  $gd = C_p G_{0v} / (\epsilon_0 G_0)$  accounts for the cell constant,  $f = x \cot(x)$ ,  $\epsilon_0$  is the dielectric constant of vacuum,  $G_{0v} = 1/376.73 [1/\Omega]$  is the characteristic conductance of vacuum, and  $G_0$  is the characteristic conductance of the line.

It is convenient to avoid using the input step wave  $V_i$  in (4), which introduce certain numerical errors due to finite rise time and limited flatness of the generated step voltage. Instead, reflection measurements on a standard specimen with known permittivity can be utilized. For two specimens, one with known permittivity  $\epsilon_s^*$ , and the other with unknown permittivity  $\epsilon_x^*$ , expression (4) can be rewritten as follows:

$$\epsilon_x^* = \frac{c}{j\omega (gd)_x} \frac{R + P_s}{RP_s + 1} f_x \quad (5)$$

where parameters  $R$  and  $P_s$  are given as:  $R = \frac{V_s(j\omega) - V_x(j\omega)}{V_s(j\omega) + V_x(j\omega)}$ ,

$P_s = \frac{j\omega (gd)_s}{cf_s} \epsilon_s^*$ , and  $f_{x,s} = x_{x,s} \cot x_{x,s}$  respectively.

In comparison to equation (4) equation (5) d simplifies the computational procedure. In addition, measurements against a standard dielectric specimen minimize the systematic uncertainty.

### III. EXPERIMENT<sup>1</sup>

The test specimens were prepared from copper-cladded dielectric films by defining  $d = 3.0$  mm diameter metal electrodes using photolithography. For such geometry the propagation length  $a = 2.47$  mm. [9]. The test methodology has been examined experimentally using a dielectric test fixture developed earlier [10]. The TDR measurements were carried out using a Tektronix TDS 8200 Digital Sampling Oscilloscope equipped with a TDR/Sampling Head. A VEE 7.0 software platform from Agilent was used for acquisition and processing of the data. Waveforms were captured in a 10 ns window containing 1024 data points with a resolution of 2.0 ps.

### IV. RESULTS AND DISCUSSION

The results of the dielectric constant measurements are illustrated in Figure 3 for dielectric films having nominal value of the dielectric constant of 3.5, 11 and 24 respectively. Figure 3a shows the dielectric constant of a 2  $\mu\text{m}$  air-gap,

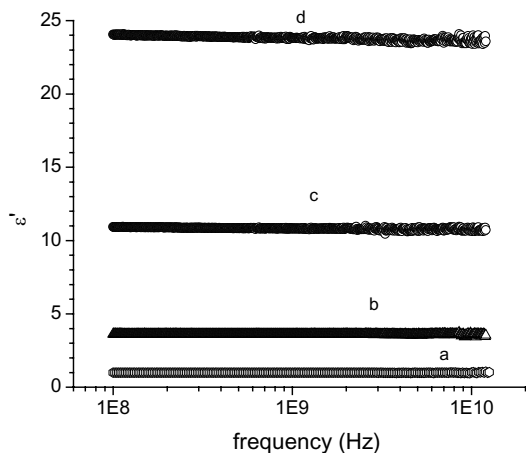


Fig. 3. – Dielectric constant,  $\epsilon'$  of film specimens measured by the TDR method (lines). (a) 2  $\mu\text{m}$  air-gap; (b) 50  $\mu\text{m}$  thick film with the nominal value of  $\epsilon'$  of 3.5; (c) 25  $\mu\text{m}$  thick film  $\epsilon'$  of 11; (d) 8  $\mu\text{m}$  thick film  $\epsilon'$  of 24.

$\epsilon_a' = 1$ , measured by the TDR from 100 MHz to about 12 GHz. In the frequency range of up to 10 GHz the relative uncertainty,  $(\Delta\epsilon_a')/\epsilon_a'$ , determined as a deviation from the standard value of 1.00 is below 5 %. The combined uncertainty for the dielectric loss,  $\Delta\epsilon_a''$ , is estimated to be less than 0.01 in the same frequency range. At higher frequencies, above 10 GHz the uncertainty increases to about 5 % due to irreproducible behavior of the test fixture that could not be compensated by the calibration procedure. Our measurement method fails to provide accurate results above 12 GHz. The difficulties in that range originate from the instrumental limits in the voltage step generation, timing, and waveform detection.

The experimental error in permittivity measurements for an unknown specimen can be minimized to the level indicated above for the air-gap if the TDR response of the unknown specimen follows that of the standard. In practice, the measured waveform differs from that of the standard and the uncertainty in the measured permittivity is larger due to uncompensated electrical noise errors such as the time and the amplitude jitter, and errors resulting from the time-to-frequency conversion. It has been determined that the combined uncertainty,  $\Delta\epsilon_x^*$ , for an unknown specimen can be evaluated using the relaxation charging time,  $T$  (see equation 1), as an indicator of deviation from the standard behavior. If the value of complex permittivity for the standard sample has uncertainty  $\Delta\epsilon_s^*$ , the uncertainty  $\Delta\epsilon_x^*$  for the unknown specimen can be obtain from expression (6).

$$\Delta\epsilon_x^* = \Delta\epsilon_s^* \times 10^{|\log(T_x/T_s)|} \quad (6)$$

where  $T_x$  is the relaxation charging time for the unknown sample and  $T_s$  denotes the relaxation charging time for the standard. The dielectric permittivity results for an organic

<sup>1</sup>Certain equipment, instruments or materials are identified in this paper in order to adequately specify the experimental details. Such identification does not imply recommendation by the National Institute of Standards and Technology nor does it imply the materials are necessarily the best available for the purpose.

resin film, and two BaTiO<sub>3</sub> filled high dielectric composite films are shown in Figure 3b, 3c and 3d. At 5 GHz the permittivity of the materials (b), (c) and (d) is:  $\epsilon_b^*=(3.6 - j0.01)$ ,  $\epsilon_c^*=(10.8 - j0.024)$  and  $\epsilon_d^*=(23.8 - j0.03)$  respectively. The relative uncertainty of measurements obtained from equation (6) for the specimens (b) and (c) is about 5 %, and for the specimen (d) the uncertainty is within 8 %. It is seen that the TDR results agree rather well with the permittivity nominal values.

The upper frequency limit in the TDR measurements shown in Figure 3 is related to resonance conditions in the dielectric film [9]. The multiple reflection pattern resulting from wave propagation in the specimen section has been observed directly on the TDR waveform using a high dielectric constant film (Figure 4).

The time between consecutive reflections is about 60 ps, which for the dielectric constant of 36 corresponds to the propagation length,  $a$ , of about 2.47 mm. This experimental result reaffirms the correctness of the fundamental approach behind the equation (5). In comparison to the lumped element approximation, the presented methodology provides more

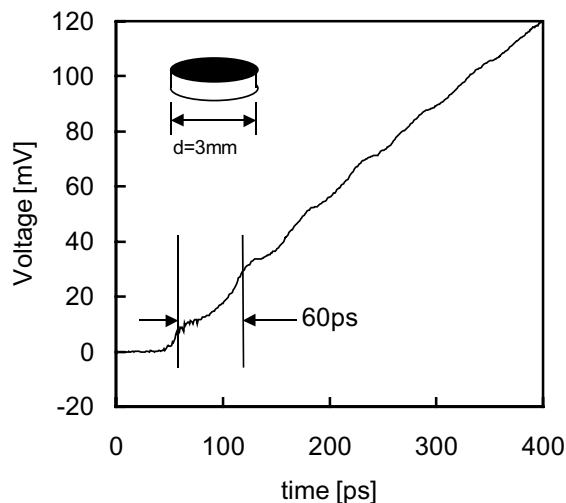


Figure 4 – Propagation delay of 60 ps is superimposed on the TDR waveform of the film specimen having diameter of 3 mm and the value of the dielectric constant of 36.

accurate results at higher frequencies, especially for high dielectric constant films.

## V. CONCLUSION

A time-domain reflectometry technique has been developed to measure permittivity of dielectric films in the broad frequency range including the microwave. The technique can utilize an air-gap, or any dielectric film of known permittivity as a reference to minimize the systematic uncertainty.

In order to account for wave propagation in the specimen section, a working equation has been delivered to account for

the propagation in the specimen section. In comparison to the previously developed lumped element approximations, the presented methodology provides more accurate results at higher frequencies, especially for high dielectric constant films.

The technique has been evaluated at frequencies from 100 MHz to 10 GHz using several polymer composite films, 8  $\mu$ m to 100  $\mu$ m thick, having the dielectric constant ranging from 3.5 to 40. The results obtained in the broad frequency range by the TDR compared well with those obtained at discrete resonant frequencies. In comparison to other techniques, TDR provides a more intuitive and direct insight into capacitance density and impedance characteristics, which is useful in high-frequency characterization of materials for embedded capacitance applications.

## ACKNOWLEDGMENT

This report is based in part upon work supported by the NIST Advanced Technology Program.

## REFERENCES

- [1] ASTM D150, D669, IPC TM-650, 2.5.5.1-9, "Permittivity (dielectric constant) and loss tangent (dissipation factor) of insulating materials", Rev. 5/86.
- [2] ASTM 3380, IPC TM-650, 2.5.5.5, "Stripline test for complex permittivity of circuit board materials to 14 GHz", Rev. 5/97.
- [3] M. A. Saed, "Measurement of the Complex Permittivity of Low-Loss Planar Microwave Substrates using Aperture-Coupled Microstrip Resonators", IEEE Trans. Microwave Theory Meas., Vol. MTT 41, pp. 1343-1348, 1993.
- [4] Y. Kantor, "Dielectric constant measurements using printed circuit techniques at microwave frequencies", Proceedings of the Mediterranean Electrotechnical Conference - MELECON. Part 1 (of 2) May 18-20 1998, Tel-Aviv, Israel, Vol. 1 pp. 101-105, 1998, Sponsored by: IEEE Piscataway NJ USA.
- [5] C. D. Gupta, "A new microwave method of measuring complex dielectric constant of high-permittivity thin films", IEEE Trans. Instrum. Meas., Vol. IM 24, pp. 61-65, 1975.
- [6] D. Galt and J. C. Price, "Ferroelectric thin film characterization using superconducting microstrip resonators", IEEE Trans. Appl. Supercond., Vol. 5, pp. 2575-2578, 1995.
- [7] N. G. Paulter, "A fast and accurate method for measuring the dielectric constant of printed wiring board materials", IEEE Trans. Comp., Pack., Manuf., Techn., Vol. 19, pp. 214-225, 1996.
- [8] M. A. Stuchly and S. S. Stuchly "Coaxial-line-reflection methods for measuring dielectric properties of biological substances at radio and microwave frequencies" IEEE Trans. Instrum. Meas., Vol. IM 29, pp. 176-183, 1980.
- [9] J. Obrzut, A. Anopchenko, "Input Impedance of a Coaxial Line Terminated with a Complex Gap Capacitance – Numerical and Experimental Analysis," IEEE Trans. Instrum. Meas., vol. 53, pp. 1197-1202, 2004.
- [10] J. Obrzut, A. Anopchenko and R. Nozaki, "Broadband permittivity measurements of high dielectric constant films, IEEE IMTC-05 Conference Proceedings, Vol. 2, pp. 1350 – 1353, 2005.